Clinical presentations and skin denervation in amyloid neuropathy due to transthyretin Ala97Ser

N.C.-C. Yang, MS*
M.-J. Lee, MD, PhD*
C.-C. Chao, MD*
Y.-T. Chuang, MS
W.-M. Lin, MS
M.-F. Chang, MS
P.-C. Hsieh, BS
H.-W. Kan, BS
Y.-H. Lin, BS
C.-C. Yang, MD
M.-J. Chiu, MD, PhD
H.-H. Liou, MD, PhD
S.-T. Hsieh, MD, PhD

Address correspondence and reprint requests to Dr. Sung-Tsang Hsieh, Department of Neurology, National Taiwan University Hospital, 7 Chung-Shan S. Road, Taipei 10002, Taiwan
shsieh@ntu.edu.tw

ABSTRACT

Objective: Familial amyloid polyneuropathy (FAP) due to amyloidogenic transthyretin (TTR) is often associated with impairment of thermonociceptive functions. This study investigated skin innervation and its clinical significance in genetically defined FAP due to a hot-spot Ala97Ser TTR mutation (Ala97Ser).

Methods: Skin biopsies were performed on the distal leg of patients with Ala97Ser, and intraepidermal nerve fiber (IENF) densities were quantified.

Results: There were 19 unrelated patients with Ala97Ser manifesting a late-onset (59.47 ± 5.70 years) generalized neuropathy with disabling motor, sensory, and autonomic symptoms. Against a background of a slowly progressive course, 7 patients (36.8%) exhibited additional rapid declines in neurologic deficits, which were associated with elevation of the protein content in the CSF ($p < 0.001$). The IENF density was markedly reduced in Ala97Ser patients compared to age- and gender-matched controls (0.99 ± 1.11 vs 8.31 ± 2.87 fibers/mm, $p < 0.001$). Skin denervation was present in all patients and was lower in patients with a higher disability grade (0.17 ± 0.26 vs 1.37 ± 1.16 fibers/mm, $p = 0.003$). Albuminocytologic dissociation in the CSF was observed in 14 patients (73.7%), and the IENF density was negatively correlated with the CSF protein concentration ($p = 0.015$).

Conclusions: Skin denervation was common in Ala97Ser, and degeneration of cutaneous nerve terminals was correlated with the severity of clinical phenotypes and the level of CSF protein.
Neurology® 2010;75:532–538

GLOSSARY

CMAP = compound muscle action potential; **FAP** = familial amyloid polyneuropathy; **H-E** = hematoxylin-eosin; **IENF** = intraepidermal nerve fiber; **NCS** = nerve conduction studies; **RFLP** = restriction fragment length polymorphism; **TTR** = transthyretin.

Familial amyloid polyneuropathy (FAP) due to mutations of transthyretin (TTR) has a worldwide distribution, with particularly high prevalences in Portugal, Japan, and Sweden.[1-4] FAP is characterized by motor, sensory, and autonomic symptoms.[5-7] Among TTR mutations associated with FAP, Val30Met is the most common form in various ethnic populations.[2,8,9] One report documented Ala97Ser mutation as cause of adult-onset FAP in Taiwan.[10] However, the phenotypes of Ala97Ser mutation-related FAP including clinical manifestations, disease course, neurophysiology, and neuropathology have not been explored in detail.

Neuropathic pain and reduced sensations to thermonociceptive stimuli are major presentations of TTR mutation-related FAP.[11,12] These observations imply the potential involvement of small-diameter sensory nerves in addition to the loss of large myelinated sensory nerves.[13-15] By measuring the intraepidermal nerve fiber (IENF) density, the degree of skin innervation can be quantified as evidence of small-fiber sensory neuropathy.[16-20] The IENF density is also correlated with functional parameters of neuropathy in addition to serving as an index of small-fiber

Supplemental data at www.neurology.org

*These authors contributed equally to this work.

From the Departments of Anatomy and Cell Biology (N.C.-C.Y., W.-M.L., M.-F.C., H.-W.K., S.-T.H.), Medicine (P.-C.H.), and Pharmacology (H.-H.L.), National Taiwan University College of Medicine, Taipei; and Departments of Neurology (M.-J.L., C.-C.C., Y.-H.L., C.-C.Y., M.-J.C., H.-H.L., S.-T.H.) and Medical Genetics (Y.-T.C.), National Taiwan University Hospital, Taipei, Taiwan.

Study funding: Supported by the National Health Research Institute, Taiwan (NHRI-EX98-9736NI), the National Science Council, Taiwan (NSC97-2320-B-002-042-MY3), and the Excellent Translational Medicine Research Projects of NTUMC and NTUH (98C101-201).

Disclosure: Author disclosures are provided at the end of the article.

sensory neuropathy, for example, thermal thresholds.[17,21] In diabetic neuropathy and sarcoidosis, skin innervation is reduced with an increase in clinical severity.[22] The degree of skin denervation is correlated with microvasculitis of inflammatory neuropathies in systemic lupus erythematosus.[23] These observations suggest that skin innervation may reflect the severity of generalized disability in FAP.

We investigated genetic etiologies of adult-onset axonal polyneuropathy, and Ala97Ser appears to be a common mutation in the Taiwanese population. Herein, we reported a large cohort with a hot-spot mutation of Ala97Ser, and examined the skin innervation and its clinical significance in FAP.

METHODS

Subjects. Patients with idiopathic adult-onset axonal polyneuropathy were identified from the database of the Department of Neurology, National Taiwan University Hospital, Taipei, from January 1, 2003, to October 31, 2009. The inclusion criteria consisted of 1) length-dependent neuropathy with clinical evidence of limb weakness and sensory symptoms and 2) electrophysiologic evidence of axonal polyneuropathy on nerve conduction studies (NCS). Patients with chronic inflammatory demyelinating polyneuropathy, Guillain-Barré syndrome, multifocal motor neuropathy with conduction block, paraprotemic neuropathy, monoclonal gammopathy of undetermined significance, and concomitant systemic diseases, such as diabetes, autoimmune diseases, or malignancies (lymphoproliferative disorders, plasma cell dyscrasia), were excluded from further analysis (as detailed in e-Methods on the *Neurology*® Web site at www.neurology.org). Patients fulfilling these clinical and electrophysiologic criteria of idiopathic adult-onset axonal polyneuropathy were then subjected to genetic characterization of the Ala97Ser mutation of the human TTR gene (described below). After confirmation of a TTR mutation, the clinical and laboratory data were retrieved for analysis.

The absence of structural lesions in the gastrointestinal tract on endoscopic examination was a prerequisite to attributing gastrointestinal symptoms as the initial presentation of autonomic neuropathy. The disability grade was evaluated on a scale of 0 to VI[24] defined as grade 0, a normal neurologic status; grade I, minor signs or symptoms; grade II, able to walk without a walker or equivalent support; grade III, able to walk with a walker or support; grade IV, bedridden or chairbound; grade V, requires assisted ventilation; grade VI, deceased.

Procedures of the tests (NCS, quantitative sensory testing, autonomic function tests, genetic analysis, nerve biopsies, and skin biopsies for quantitation of epidermal innervation) followed established protocols and age- and gender-matched control subjects were retried from a previously described database.[24] All these are detailed in e-Methods.

Standard protocol approvals, registrations, and patient consents. The study was approved by the institutional review board at the National Taiwan University Hospital, Taipei, and written informed consent was obtained from all participants.

Genetic analyses of TTR mutations. Genomic DNA was extracted from the peripheral venous blood following a standard protocol. The analyses included 1) direct sequencing of the 4 exons in the entire human TTR gene (GeneID: 7276, NG 009490), 2) a high-resolution melting curve analysis, 3) restriction fragment length polymorphism (RFLP) diagnosis of the index allele, and 4) multiple sequence alignment and protein structure visualization (as detailed in e-Methods and table e-1).

Nerve biopsy. Sural nerve specimens were embedded in paraffin and stained with hematoxylin-eosin (H-E). For amyloid detection, sections were further stained with Congo red. Additional sections were immunohistochemically stained with anti-TTR antiserum (1:500, Dako, Glostrup, Denmark).

Skin biopsy and quantitation of skin innervation. A 3-mm-diameter skin punch was taken from the right distal leg 10 cm proximal to the lateral malleolus under local anesthesia with 2% lidocaine. Sections 50 μm perpendicular to the dermis were immunostained with antiserum to protein gene product 9.5 (PGP 9.5, 1:1,000; UltraClone, Isle of Wight, UK). Epidermal innervation was quantified according to established criteria in a coded fashion. The IENF density was expressed as the number of fibers/mm of epidermal length.

Statistical analysis. Numeric variables are expressed as mean ± SD, and were compared with t tests if the data followed a Gaussian distribution. If the sample size was small, numerical variables were compared using a nonparametric test (Wilcoxon rank sum test). Fisher exact test was used to compare categorical data. Correlations between variables were graphically analyzed using Stata (StataCorp LP, College Station, TX) and GraphPad Prism (GraphPad Software, San Diego, CA). Results were considered significant at $p < 0.05$.

RESULTS

Genetic characterization of the TTR gene mutation. This study identified 19 index patients with a mutation in the human TTR gene among patients who exhibited clinical and electrophysiologic evidence of idiopathic adult-onset axonal polyneuropathy. Direct sequencing of the 4 exons and the flanking intron regions of the TTR gene identified a sequence variant, c.349G>T (figure 1A). The variant showed a change in 1 amino acid from alanine to serine (p.Ala97Ser). To authenticate the pathogenic role of the sequence variant, we screened the DNA from their family members and 365 normal Taiwanese controls, and none had the Ala97Ser mutation. Using high-resolution melting curve methodology, we compared the patterns between Ala97Ser and the controls. There was a significant shift in Ala97Ser compared to the controls, suggesting the pathogenic potential of this missense mutation (figure 1B).

To verify the G>T mutation, we developed a PCR-based RFLP after digestion with the *Fok*I restriction enzyme for confirmation. In control subjects, there was only a single band of 347 bp due to the lack of a *Fok*I cutting site. In contrast, the mutated TTR harbored 2 additional bands of ~130 and ~210 bp because of the *Fok*I restriction cutting sites (figure 1C).

Figure 1 Genetic evidence of the transthyretin (TTR) mutation

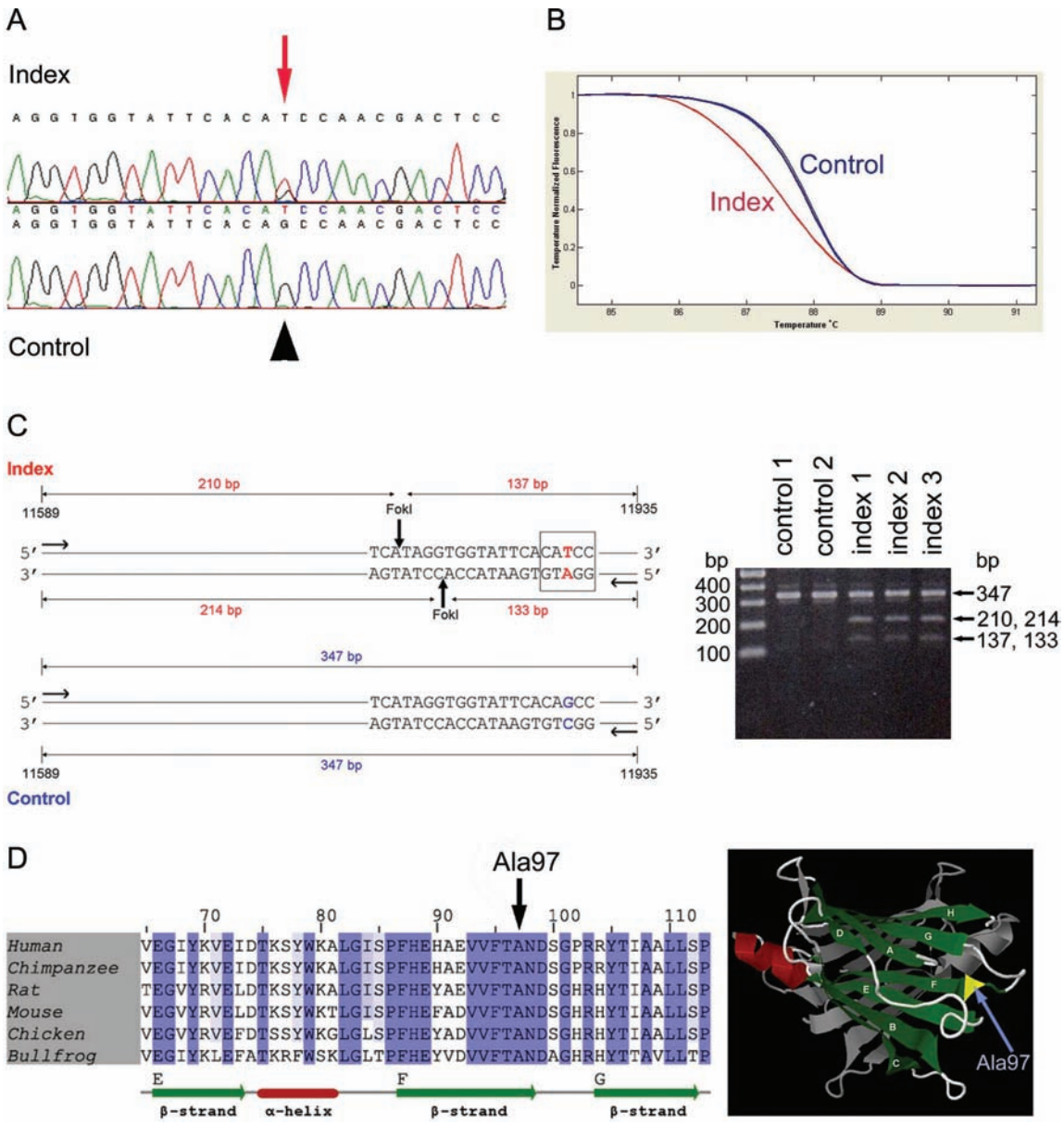

The TTR mutation was demonstrated by directly sequencing exon 4 of the human TTR gene from index patients and controls (A). The pathogenic significance of the mutation was explored with a high-resolution melting curve (B). The mutation was further confirmed by restriction fragment length polymorphism (RFLP, C). The sequence conservation of Ala97 was analyzed by bioinformatics approaches (D). (A) The sequencing chromatography of the amplicon shows a sequence variant, G (black arrowhead) replaced by a T (red arrow), which resulted in an amino acid change, Ala97Ser. (B) The high-resolution melting curve analysis for the amplicons encompassing the missense mutation reveals a lower melting curve with a substantial shift (red line) compared to the controls (dark blue lines). (C) The left panel illustrates a schematic diagram of the RFLP strategy for differentiating index and control TTR alleles. The control allele did not contain a *Fok*I cutting site and yielded a single 347-bp fragment. The index allele contained a recognition domain (boxed, CATCC), and cutting sites (arrows), for the *Fok*I restriction endonuclease and yielded 2 restriction fragments: one at ~210 bp (210,217) and the other at ~130 bp (137,133). The right panel shows the PCR-RFLP after gel electrophoresis. The controls contained only 1 band of 347 bp, while the index patients had 2 additional bands corresponding to the patterns of the restriction diagram. (D) The left panel shows a sequence alignment of TTR amino acid sequences in 6 species (human, chimpanzee, rat, mouse, chicken, and American bullfrog). The degree of conservation is indicated by the darkness of the shading. The mutation site Ala97 (blue arrow) lies in a β-pleated sheet (β-strand, green), and was conserved in all species shown here. The right panel is a molecular model of a human TTR dimer (PDB accession code: 1F41). Each TTR monomer includes 8 β-strands, labeled A through H. The amino acid residue, Ala97, shown in yellow, lies in the F-strand and is part of the hydrophobic core.

We investigated whether Ala97 was conserved by bioinformatic approaches, and this amino acid residue was conserved among several species during evolution and was located in a β-strand (figure 1D).

Clinical presentations and laboratory examinations. These 19 unrelated Ala97Ser patients (16 men and 3 women) experienced the onset of symptoms at age 59.47 ± 5.70 years (range 48–68) (table 1). The interval from

Table 1 Clinical manifestations, skin biopsy, and laboratory tests

No.	Gender	Age at onset, y/initial symptoms	Sensory symptoms[a]	Autonomic symptoms	Motor symptoms (disability grade)[b] At initial assessment	At follow-up	Interval, y	Course Chronic progression	With episode of rapid decline	CSF protein, mg/dL	IENF density, fibers/mm
1	M	56/sensory + motor	Large, small	Ortho, GI (D)	II	VI	2.5	Yes	No	37.0 (N)	3.59
2	M	57/motor (U)	Large, small	GI (C, D)	II	VI	6.0	Yes	Yes	68.0	0
3	M	48/sensory	Large, small	Ortho, GI (D), GU (R)	III	VI	8.0	Yes	No	26.8 (N)	0
4	M	65/motor	Large, small, pain	Ortho, GI (C)	III	IV	3.0	Yes	Yes	95.0	0
5	M	55/autonomic	Large, small	GI (C, D), S	II	IV	7.0	Yes	No	55.0	1.45
6	F	62/sensory	Large, small, pain	Ortho, GI (C, D), GU (I, R), S	III	IV	3.0	Yes	No	67.0	0.52
7	M	59/sensory (U)	Large, small, pain	GI (C), GU (R)	II	III	7.0[c]	Yes	No	43.0 (N)	2.67
8	M	61/sensory	Large, small, pain	Ortho, GI (C)	III	IV	3.0	Yes	Yes	96.0	0
9	M	57/sensory (U)	Large, small	Ortho, GI (C, D), S	II	III	5.0[c]	Yes	No	63.0	1.78
10	M	55/sensory + motor	Large, small	Ortho, GI (C, D)	II	IV	6.0	Yes	No	64.0	0.67
11	M	56/autonomic	Large, small, pain	Ortho, GI (D)	II	IV	5.0	Yes	Yes	99.0	0
12	M	56/sensory (U)	Large, small, pain	GI (C, D)	II	IV	5.0	Yes	No	57.4	0.41
13	M	66/sensory (U)	Large, small, pain	Ortho, GI (D)	III	IV	6.0	Yes	Yes	52.0	0.5
14	M	51/autonomic	Large, small, pain	Ortho, GI (C, D)	II	III	9.0[c]	Yes	No	60.3	2.41
15	F	67/sensory (U)	Large, small, pain	GI (C), S	II	III	6.0[c]	Yes	No	40.4 (N)	0.86
16	F	68/sensory	Large, small, pain	Ortho, GI (D), GU (I)	III	IV	4.0	Yes	Yes	67.8	0
17	M	61/sensory (U)	Large, small	Ortho, GI (C), S	II	III	3.75[c]	Yes	No	49.7	2.27
18	M	61/sensory	Large, small	Ortho, GI (C, D), GU (I)	II	VI	5	Yes	Yes	88	0
19	M	68/sensory + motor	Large, small, pain	Ortho, GU (I)	II	II	2.5[c]	Yes	No	44.3 (N)	1.65
Summary		Sensory: 11	Large (100%)	GI (94.7%)	Grade II: 13	Grade II: 1		100%	36.8%	73.7%[d]	100%[d]
		Motor: 2	Small (100%)	Ortho (73.7%)	Grade III: 6	Grade III: 5					
		Sensory + motor: 3	Pain (57.9%)	GU (31.6 %)		Grade IV: 9					
		Autonomic: 3		S (26.3%)		Grade VI: 4					

Abbreviations: C = constipation; D = diarrhea; GI = gastrointestinal symptoms; GU = genitourinary symptoms; I = urinary incontinence; IENF = intraepidermal nerve fiber; N = normal; Ortho = orthostatic hypotension; R = urine retention; S = sudomotor failure symptoms, i.e., anhidrosis or hypohidrosis of the feet; U = upper extremities.

[a] Large = sensory symptoms due to large-fiber deficits; Small = sensory symptoms due to small-fiber deficits.

[b] Motor symptoms at follow-up, according to the last follow-up; Interval, the interval between the onset of symptoms to being wheelchair-bound (grade = IV), for those patients with a disability grade ≥IV at the follow-up.

[c] The interval between the onset of the symptoms to the last follow-up with a disability grade of II or III at the last follow-up.

[d] Abnormal rate.

symptoms onset to disability grade VI in 14 patients was 4.71 ± 1.76 years (range 2.5–8). In summary, all patients had generalized disabling neuropathy and eventually all experienced motor, sensory, and autonomic symptoms. Sensations of large and small fibers were impaired to similar degrees, i.e., sensory ataxia and a loss of sensation to thermal stimuli.

NCS, quantitative sensory testing, and autonomic function tests showed 1) axonal-type sensorimotor polyneuropathy, 2) elevated vibratory and thermal thresholds, 3) the absence of a sympathetic skin response, and 4) reduced R-R interval variability, consistent with the impairment of motor, sensory, and autonomic functions (detailed in table e-2).

All patients followed a chronic progressive course with a gradual increase in neurologic deficits. Within 2.5–8 years, the motor deficits became so evident that patients required a wheelchair for ambulation. Seven patients had 1 or more episodes of rapid deterioration which developed within weeks (ranging from 1 week to 3 months). Six patients experienced aggravation of weakness leading to an increase on the disability scale and impairments of hand functions. One had marked gastrointestinal dysautonomia and re-

quired nasogastric intubation for nutrition. In the 6 patients with rapid motor decline, 4 patients had significant reductions in the amplitudes of compound muscle action potentials (CMAP) on NCS. CMAP was absent in 1 patient before the acute episode, and 1 patient had her first NCS during the acute episode. There was no evidence of conduction block in any of these 6 patients. These 6 patients received immunomodulating therapy including plasma exchange (4 cases), steroid therapy (1), and IV immunoglobulin (1). Only 1 patient had some improvement after plasma exchange (a reduction in the neurologic disability score from 79 to 56).

On CSF studies, 14 patients (73.7%) had an elevated protein level, but none had pleocytosis. The protein level was higher in the 7 patients with episodes of rapid deterioration on a background of a chronic progressive course than in the other patients without such episodes (80.8 ± 18.2 vs 50.7 ± 12.5 mg/dL, $p < 0.001$).

TTR in amyloids of nerve biopsies. The pathology of FAP was demonstrated as an eosinophilic deposition of amyloid in biopsy specimens from 15 of 19 patients: 13 in the sural nerves, 1 in the kidney, and 1 in the abdominal subcutaneous fat tissue. Amyloid deposition appeared as amorphous aggregates surrounding vascular walls on H-E–stained paraffin sections, which was confirmed by Congo red staining. The presence of TTR in the amyloid was further demonstrated by immunohistochemistry with an anti-TTR antibody. On semithin sections, the sural nerves showed a pattern of axonal degeneration with significant loss of large and small myelinated nerve fibers (figure e-1).

Figure 2 **Quantitation of skin innervation in familial amyloid polyneuropathy due to mutated transthyretin (Ala97Ser)**

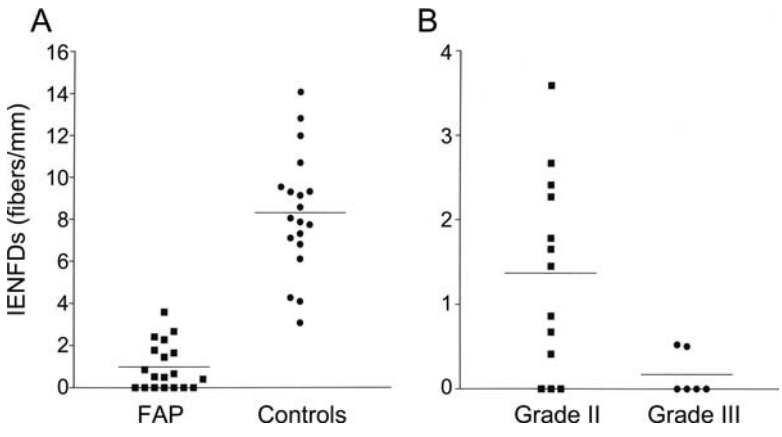

(A) The intraepidermal nerve fiber densities (IENFDs) were reduced in the Ala97Ser group compared to the age- and gender-matched control group. (B) The IENFDs were related to the disability grade at the time of the biopsy.

Skin denervation. In the control skin, varicose IENFs were apparent in the epidermis. Dermal nerve fibers formed dense bundles, and the secretory coils were surrounded by dense nerve fibers in control sweat glands. In Ala97Ser skin, IENFs were almost entirely depleted, and only sparse dermal nerve fibers with a fragmented appearance were observed. The coils of sweat glands were surrounded by residual immunoreactive dots, which reflected degenerated nerve fibers (figure e-2).[25,26]

The IENF density in the Ala97Ser group (table 1) was markedly reduced compared to the age- and gender-matched control group (0.99 ± 1.11 vs 8.31 ± 2.87 fibers/mm, $p < 0.001$, figure 2A) with all patients (100%) exhibiting reduced IENF density (table 1). We further explored the clinical significance of skin denervation. The IENF density was lower in patients unable to walk independently (i.e., disability grade ≥III) than in those who could independently walk (i.e., disability grade II) at the time of the skin biopsy (0.17 ± 0.26 vs 1.37 ± 1.16 fibers/mm, $p = 0.003$, figure 2B). The IENF density was negatively correlated with the protein concentration of the CSF, i.e., a lower IENF density was associated with a higher CSF protein concentration (slope = −0.029 ± 0.011, $p = 0.015$). For thermal sensations, the IENF density was linearly correlated with the cold threshold of the toe (slope = 0.059 ± 0.019, $p = 0.009$).

DISCUSSION This study demonstrates that the missense mutation, Ala97Ser, of the TTR gene results in a late-onset generalized disabling neuropathy involving all components of the peripheral nerves: motor, sensory, and autonomic nerves,[4,6,7,27] which leads to the loss of independent ambulation in 2.5–8 years after the onset of neuropathy. All patients developed insidious onset of motor, sensory, and autonomic symptoms. Dysautonomic symptoms, such as chronic diarrhea, might occur earlier in the course of FAP, and warrant caution to avoid a delay in the diagnosis.

Additionally, patients with the TTR mutation, Ala97Ser, develop unique and characteristic clinical features compared to those with the most common one, Val30Met. First, almost all Ala97Ser patients had a late age at onset (>50 years of age), while Val30Met patients had both early- and late-onset types.[1] Second, previous studies on FAP emphasized a chronic progressive course.[2,6,28] Nevertheless, 36.8% of patients with the TTR Ala97Ser mutation had episodes of rapid deterioration associated with albuminocytologic dissociation. This may be attributed to the inherent nature of the mutation or implies the possibility of a superimposed inflammatory

neuropathy. Further large surveys of FAP patients with other mutations are necessary to ascertain this correlation between the genotype and phenotype.

Several lines of evidence in our report suggest that Ala97Ser is pathogenic.[9] First, the mutated TTR (Ala97Ser) was absent from 365 normal Taiwanese controls, and the mutated allele had a different pattern on the high-resolution melting curve analysis. In addition, the alanine residue at position 97 was found to have been highly conserved among various species during evolution. Moreover, we demonstrated the presence of the TTR protein in amyloid deposits on sural nerve biopsies.

This hospital-based study suggests that Ala97Ser may be a significant genetic etiology for chronic panmodality polyneuropathy of adult onset compared to other mutations in Taiwan. This observation warrants systematic screening studies for Ala97Ser in Taiwanese patients with adult-onset idiopathic chronic polyneuropathy. Several theories attempted to elucidate the pathogenesis of the mutated TTR in FAP, mainly for Val30Met.[29-31] Further studies are required to understand whether the Ala97Ser mutation shares a similar mechanism of amyloid deposits.

Skin denervation is a leading manifestation in patients with the Ala97Ser TTR mutation (100%), indicating that small-fiber sensory neuropathy is one of the most prevalent components of FAP compared to other types of neuropathy, such as diabetic neuropathy,[21,32-34] Guillain-Barré syndrome,[24] and neuropathy associated with systemic lupus erythematosus and autoimmune diseases.[23,35-38] The frequencies of small-fiber sensory neuropathy in the aforementioned neuropathies range from 60%–80%. In contrast, IENF densities were reduced in all patients with the Ala97Ser mutation, and all of these patients were symptomatic.

An intriguing observation is the concordance of skin denervation with ambulation difficulty and increased CSF protein. The quantitative assessment of cutaneous nerve fibers can be employed as an indicator of the severity of the neuropathy; for example, the IENF density was associated with the disability grade in Guillain-Barré syndrome and eosinophilia-associated neuropathy.[24,38] The protein content in the CSF was elevated in 73.7% of patients with the Ala97Ser TTR mutation, and there was a trend toward greater skin denervation for those patients with a higher CSF concentration of the protein. This finding suggests that the enhanced transudation of proteins to the CSF[39,40] or the concomitant presence of immune-mediated neuropathy[24,40] may be deleterious to small-diameter sensory nerves, which leads to skin denervation. These correlations provide a foundation for further large-scale studies to explore the significance in FAP on skin innervation due to other TTR mutations.

AUTHOR CONTRIBUTIONS

Statistical analysis was conducted by Dr. C.-C. Chao.

DISCLOSURE

N.C.-C. Yang and Dr. Lee report no disclosures. Dr. Chao receives research support from the National Science Council. Y.-T. Chuang, W.-M. Lin, M.-F. Chang, P.-C. Hsieh, H.-W. Kan, Y.-H. Lin, Dr. Yang, Dr. Chiu, and Dr. Liou report no disclosures. Dr. Hsieh serves as an Associate Editor of *Acta Neurologica Taiwanica* and on the editorial board of the *Journal of Clinical Neuroscience* and receives research support from the National Health Research Institute, Taiwan, the National Science Council, Taiwan, and the Excellent Translational Medicine Research Projects of National Taiwan University College of Medicine and National Taiwan University Hospital.

Received December 7, 2009. Accepted in final form April 27, 2010.

REFERENCES

1. Koike H, Misu K, Sugiura M, et al. Pathology of early- vs late-onset TTR Met30 familial amyloid polyneuropathy. Neurology 2004;63:129–138.
2. Ando Y, Nakamura M, Araki S. Transthyretin-related familial amyloidotic polyneuropathy. Arch Neurol 2005;62:1057–1062.
3. Misu Ki, Hattori N, Nagamatsu M, et al. Late-onset familial amyloid polyneuropathy type I (transthyretin Met30-associated familial amyloid polyneuropathy) unrelated to endemic focus in Japan: clinicopathological and genetic features. Brain 1999;122:1951–1962.
4. Reilly MM, Adams D, Booth DR, et al. Transthyretin gene analysis in European patients with suspected familial amyloid polyneuropathy. Brain 1995;118:849–856.
5. Zanette G, Cacciatori C, Tamburin S. Central sensitization in carpal tunnel syndrome with extraterritorial spread of sensory symptoms. Pain 2010;148:227–236.
6. Reilly M. Hereditary amyloid neuropathy. In: Dyck PJ, Thomas PK, eds. Peripheral Neuropathy, 4th ed. Philadelphia, PA: Elsevier Saunders; 2005:1921–1936.
7. Thomas PK, King RHM. Peripheral nerve changes in amyloid neuropathy. Brain 1974;97:395–406.
8. Sousa MM, Saraiva MJ. Neurodegeneration in familial amyloid polyneuropathy: from pathology to molecular signaling. Prog Neurobiol 2003;71:385–400.
9. Plante-Bordeneuve V, Ferreira A, Lalu T, et al. Diagnostic pitfalls in sporadic transthyretin familial amyloid polyneuropathy (TTR-FAP). Neurology 2007;69:693–698.
10. Liu YT, Lee YC, Yang CC, Chen ML, Lin KP. Transthyretin Ala97Ser in Chinese-Taiwanese patients with familial amyloid polyneuropathy: genetic studies and phenotype expression. J Neurol Sci 2008;267:91–99.
11. Hou X, Aguilar MI, Small DH. Transthyretin and familial amyloidotic polyneuropathy. Recent progress in understanding the molecular mechanism of neurodegeneration. FASEB J 2007;274:1637–1650.
12. Adams D, Samuel D, Goulon-Goeau C, et al. The course and prognostic factors of familial amyloid polyneuropathy after liver transplantation. Brain 2000;123:1495–1504.
13. Kennedy WR, Said G. Sensory nerves in skin: answers about painful feet? Neurology 1999;53:1614–1615.
14. Oaklander AL, Fields HL. Is reflex sympathetic dystrophy/complex regional pain syndrome type I a small-fiber neuropathy? Ann Neurol 2009;65:629–638.

15. Mendell JR, Sahenk Z. Painful sensory neuropathy. N Engl J Med 2003;348:1243–1255.
16. Ebenezer GJ, McArthur JC, Thomas D, et al. Denervation of skin in neuropathies: the sequence of axonal and Schwann cell changes in skin biopsies. Brain 2007;130: 2703–2714.
17. Devigili G, Tugnoli V, Penza P, et al. The diagnostic criteria for small fibre neuropathy: from symptoms to neuropathology. Brain 2008;131:1912–1925.
18. Gibbons CH, Griffin JW, Polydefkis M, et al. The utility of skin biopsy for prediction of progression in suspected small fiber neuropathy. Neurology 2006;66:256–258.
19. Herrmann DN, Griffin JW, Hauer P, Cornblath DR, McArthur JC. Epidermal nerve fiber density and sural nerve morphometry in peripheral neuropathies. Neurology 1999;53:1634–1640.
20. Ebenezer GJ, Hauer P, Gibbons C, McArthur JC, Polydefkis M. Assessment of epidermal nerve fibers: a new diagnostic and predictive tool for peripheral neuropathies. J Neuropathol Exp Neurol 2007;66:1059–1073.
21. Shun CT, Chang YC, Wu HP, et al. Skin denervation in type 2 diabetes: correlations with diabetic duration and functional impairments. Brain 2004;127:1593–1605.
22. Quattrini C, Jeziorska M, Boulton AJM, Malik RA. Reduced vascular endothelial growth factor expression and intra-epidermal nerve fiber loss in human diabetic neuropathy. Diabetes Care 2008;31:140–145.
23. Tseng MT, Hsieh SC, Shun CT, et al. Skin denervation and cutaneous vasculitis in systemic lupus erythematosus. Brain 2006;129:977–985.
24. Pan CL, Tseng TJ, Lin YH, Chiang MC, Lin WM, Hsieh ST. Cutaneous innervation in Guillain-Barré syndrome: pathology and clinical correlations. Brain 2003;126:386–397.
25. Hsieh ST, Chiang HY, Lin WM. Pathology of nerve terminal degeneration in the skin. J Neuropathol Exp Neurol 2000;59:297–307.
26. Hsieh YL, Chiang H, Tseng TJ, Hsieh ST. Enhancement of cutaneous nerve regeneration by 4-methylcatechol in resiniferatoxin-induced neuropathy. J Neuropathol Exp Neurol 2008;67:93–104.
27. Kim DH, Zeldenrust SR, Low PA, Dyck PJ. Quantitative sensation and autonomic test abnormalities in transthyretin amyloidosis polyneuropathy. Muscle Nerve 2009;40: 363–370.
28. Benson MD, Kincaid JC. The molecular biology and clinical features of amyloid neuropathy. Muscle Nerve 2007; 36:411–423.
29. Sebastiao MP, Lamzin V, Saraiva MJ, Damas AM. Transthyretin stability as a key factor in amyloidogenesis: x-ray analysis at atomic resolution. J Mol Biol 2001;306:733–744.
30. Cardoso I, Brito M, Saraiva MJ. Extracellular matrix markers for disease progression and follow-up of therapies in familial amyloid polyneuropathy V30M TTR-related. Dis Markers 2008;25:37–47.
31. Santos SD, Magalhaes J, Saraiva MJ. Activation of the heat shock response in familial amyloidotic polyneuropathy. J Neuropathol Exp Neurol 2008;67:449–455.
32. Kennedy WR, Wendelschafer-Crabb G, Johnson T. Quantitation of epidermal nerves in diabetic neuropathy. Neurology 1996;47:1042–1048.
33. Polydefkis M, Hauer P, Sheth S, Sirdofsky M, Griffin JW, McArthur JC. The time course of epidermal nerve fibre regeneration: studies in normal controls and in people with diabetes, with and without neuropathy. Brain 2004;127: 1606–1615.
34. Boucek P, Havrdova T, Voska L, et al. Epidermal innervation in type 1 diabetic patients: a 2.5-year prospective study after simultaneous pancreas/kidney transplantation. Diabetes Care 2008;31:1611–1612.
35. Omdal R, Mellgren SI, Goransson L, et al. Small nerve fiber involvement in systemic lupus erythematosus: a controlled study. Arthritis Rheum 2002;46:1228–1232.
36. Goransson LG, Brun JG, Harboe E, Mellgren SI, Omdal R. Intraepidermal nerve fiber densities in chronic inflammatory autoimmune diseases. Arch Neurol 2006;63:1410–1413.
37. Goransson LG, Tjensvoll AB, Herigstad A, Mellgren SI, Omdal R. Small-diameter nerve fiber neuropathy in systemic lupus erythematosus. Arch Neurol 2006;63:401–404.
38. Chao CC, Hsieh ST, Shun CT, Hsieh SC. Skin denervation and cutaneous vasculitis in eosinophilia-associated neuropathy. Arch Neurol 2007;64:959–965.
39. Hadden RDM, Hughes RAC. Management of inflammatory neuropathies. J Neurol Neurosurg Psychiatry 2003; 74:ii9–ii14.
40. Thompson EJ. Different blood-CSF barriers. In: Thompson EJ, ed. Proteins of the Cerebrospinal Fluid: Analysis and Interpretation in the Diagnosis and Treatment of Neurological Disease, 2nd ed. Amsterdam: Elsevier; 2005:43–63.

Supplementary Methods

Characterization of patients

The patients with chronic inflammatory demyelinating polyneuropathy,[1] Guillain-Barré syndrome,[2] multifocal motor neuropathy with conduction block,[3-6] paraprotemic neuropathy, monoclonal gammopathy of undetermined significance (MGUS),[7] were excluded for further analysis by the clinical course, the findings on nerve conduction studies, and laboratory tests. Patients with concomitant systemic diseases such as diabetes mellitus, chronic kidney disease, thyroid diseases, syphilis, human immunodeficiency virus infection, paraproteinemia, autoimmune diseases, malignancies (lymphoproliferative disorders, plasma cell dyscrasia, et al.), history of using neurotoxic medications (such as chemotherapeutic agents), alcoholism, or toxin exposure were also excluded by detailed history, physical check-ups, neurological examinations, and relevant laboratory tests including hematological, biochemical, endocrine, infection, malignancy, nutritional and autoimmune profiles (plasma glucose level, HbA1C, triglyceride, cholesterol, liver enzymes, blood urea nitrogen, creatinine, uric acid, vitamain B12 level, folic acid, serum immunofixation electrophoresis, immunoglobulin profiles of IgG, IgA, IgM, and kappa/lambda light chain proteins, antinuclear antibody, rheumatoid factor, anti-Sjögren syndrome A antigen, anti-Sjögren syndrome B antigen, anti-Smith antigen, and anti-scleroderma antigen, SCL-70, anti-ganglioside GM1 antibodies, and tumor markers).

Nerve conduction studies

Nerve conduction studies were performed with a Nicolet (Madison, WI) Viking IV Electromyographer on all patients following standardized methods. The amplitude of the sural sensory action potential (sural SAP) and the amplitude of compound muscle action potentials on distal stimulation (CMAP) from the peroneal nerve were analyzed.

Quantitative sensory testing

We performed quantitative sensory testing with a Thermal Sensory Analyzer and Vibratory Sensory Analyzer (Medoc Advanced Medical System, Minneapolis, MN) to measure sensory thresholds of warm, cold, and vibratory sensations as reported before.[8] The stimulator was applied to the skin of the big toe. The examiner explained the procedures to the subjects, and the subjects made several trials to become familiar with the test. For the measurement of thermal threshold temperatures, reference temperatures were set to 32 °C. We used two testing strategies: the method of limits and the method of level. The results of these two algorithms were correlated and the thresholds for the method of level were presented here. The method of

level was independent of reaction time, and the results of this algorithm are presented in this report. Briefly, the machine delivered a stimulus of constant intensity which had been determined by the algorithm. The intensity of the next stimulus was either increased or decreased by a fixed ratio according to the response of the subject i.e., whether or not the subject perceived the stimulus. Such procedures were repeated until a pre-determined difference of intensity was reached. The mean intensity of the last two stimuli was the threshold for the level method. Thermal thresholds were expressed as warm threshold temperature and cold threshold temperature. These temperatures were compared with normative values for age. Vibratory thresholds were measured with similar algorithms, and expressed in micrometers.

Autonomic function tests

R-R interval variability (RRIV) for the cardiac-vagal function and sympathetic skin response (SSR) for the sudomotor function were performed following established protocol by using Nicolet Viking IV Electromyographer (Madison, WI). RRIV was obtained during rest position and forced deep breathing. Each test was repeated for three times and the mean value was compared with that for the age-matched controls in our laboratory.[9] SSR was recorded in the palm and sole, and the results were interpreted as present or absent but were not evaluated quantitatively because of variations in the latencies and amplitudes of SSR. Medication that interfered with sympathetic or parasympathetic functions was not administered before or during these tests.

Sequencing of the human TTR gene (GeneID: 7276, NG_009490)

Genomic DNA was extracted from the peripheral venous blood following a standard protocol. Four exons and their flanking intron regions of the human TTR gene were amplified by polymerase chain reaction (PCR) (primer sequences in the Supplementary Table 1). In each reaction, we added 50~100 ng of genomic DNA and 1 U of Thermo-Start Taq DNA polymerase (ABgene, Epsom, Surrey, UK). The PCR conditions were as follows: initially the genomic DNA was denatured at 95 °C for 15 min followed by 30 cycles of amplification. Each cycle was composed of denaturation at 95 °C for 30 s, annealing at an optimal temperature (listed in the Supplementary Table) for 30 s, and amplification at 72 °C for 45 s. The final step for amplification was at 72 °C for 7 min. The amplicons were then purified using the Gel/PCR DNA Fragments Extraction Kit (Geneaid, Taipei, Taiwan) and subjected to direct sequencing. Sequencing was performed at the corresponding exons using the ABI3730

automatic DNA sequencer (Applied Biosystems, Foster City, CA).

Supplementary Table 1. Primer sequences used to amplify the exons and flanking intron regions of the human TTR gene

Exon	Primer	Sequences of primers	Amplicon Size (bp)	Annealing Temperature (°C)
1	TTR-1F	TCAATAATCAGAATCAGCAG	395	57
	TTR-1R	ATGCTCAGAGTTCAAGTCC		
2	TTR-2F	TGTAATTCTTGTTTCGCTC	418	59
	TTR-2R	TCCTGGTCACTTCCTAGC		
3	TTR-3F	CTTCTGACTTAGTTGAGGG	438	57
	TTR-3R	TGTATAATAGGAAAGGGAAC		
4	TTR-4F	TAATTAAGTTGGCACTGG	466	57
	TTR-4R	CTGCCCAGATACTTTCTAG		

F: forward; R: reverse

High-resolution melting curve

Two newly designed primers were employed to amplify a fragment of 88 bp by a primer set (forward primer, GGGCTCTGGTGGAAATGG and reverse primer, GGCAATGGTGTAGCGGC). The protocol for the PCR was the same as that above except for supplementation of LCGreen PLUS at 1.5 μl/reaction (Idaho Technology, Salt Lake City, UT). The amplicons were then subjected to the high-resolution melting curve analysis in a LightScanner HRM machine (Idaho Technology).

Restriction fragment length polymorphism (RFLP) diagnosis of the index allele

A 347-bp fragment from DNA samples (corresponding to nucleotides 11,589~11,935 of the genomic DNA sequence for the human TTR gene with the GenBank accession no.: NG_009490) was amplified (forward primer, TGACTCTGTACTCCTGCTC and reverse primer, TTCAGGTCCACTGGAGGA), digested with the restriction endonuclease, FokI (New England Biolabs, Ipswich, MA), and analyzed on a 2% agarose gel. For the control allele, this fragment contained no FokI cutting sites and yielded a single 347-bp band. The mutated allele of the index patient containing the previously reported mutation in exon 4 of the human TTR gene (corresponding to nucleotide 11,814 of the NG_009490 sequence)[10]

created restriction cutting sites on two complementary sequences, $GGATG(N)_9$ and $CCTAC(N)_{13}$, respectively which resulted in two sets of restriction fragments of ~130 (137 and 133) and ~210 bp (210 and 214), allowing the differentiation of this allele from the control one.

Multiple sequence alignment and protein structure visualization

To determine the evolutionary conservation of the mutation site and surrounding regions, we employed ClustalW[11] to align TTR amino acid sequences from six species. Accession numbers (UniProt) were P02766 (human), Q5U7I5 (chimpanzee), P02767 (rat), P07309 (mouse), P27731 (chicken), and P31779 (American bullfrog, *Rana catesbeiana*). The output was formatted with Jalview.[12] An open-access Java viewer for chemical structures in 3D, Jmol (http://jmol.sourceforge.net/), was used to display the known crystal structure of human TTR (Protein Data Bank code 1F41).[13]

Nerve biopsy and pathological examinations

The sural nerve specimens were fixed overnight in 2% paraformaldehyde-lysine-periodate for routine histological studies and in 5% glutaraldehyde for pathological examinations, respectively. Paraffin-embedded sections at 8 μm thick were stained with hematoxylin-eosin (H&E). For amyloid detection, sections were further stained with Congo red. Additional sections were immunohistochemically stained following established protocols.[14] Briefly, sections were incubated overnight with anti-TTR antiserum (1: 500, Dako, Glostrup, Denmark) after antigen retrieval at 4 °C. After rinsing in Tris, sections were incubated with biotinylated goat anti-rabbit immunoglobulin G (IgG, Vector Laboratories, Burlingame, CA) at room temperature for 1 h and the avidinbiotin complex (Vector Laboratories) for another hour. Immunoreactive products were demonstrated with 3,3'-diaminobenzidine (Sigma, St. Louis, MO).

For nerve pathology studies, the glutaraldehyde-fixed tissues were rinsed in PB, post-fixed in 2% osmium tetraoxide for 2 h, dehydrated through a graded ethanol series, and embedded in Epon 812 resin (Polyscience, Philadelphia, PA). Semi-thin sections were cut on an ultramicrotome (Reichert Ultracut E, Leica) and stained with toluidine blue.

Skin biopsy and quantitation of skin innervation

A 3-mm-diameter skin punch was taken from the right distal leg 10 cm proximal to the lateral malleolus under local anesthesia with 2% lidocaine. The sampled skin tissue was fixed

overnight in PLP. Sections 50 μm perpendicular to the dermis were immunostained with antiserum to protein gene product 9.5 (PGP 9.5, 1: 1000; UltraClone, Isle of Wight, UK) as described in the section above for sural nerve specimens except that the reaction product was demonstrated using chromogen SG (Vector Laboratories).

Epidermal innervation was quantified according to established criteria in a coded fashion. Observers were blinded to the clinical information. PGP 9.5 (+) nerves in the epidermis of each skin section were counted at a magnification of 40x with a BX40 microscope (Olympus, Tokyo, Japan). The length of the epidermis along the upper margin of the stratum corneum in each skin section was was measured with ImageJ vers. 1.43 (Image Processing and Analysis in Java, National Institutes of Health, Bethesda, MD: http://rsbweb.nih.gov/ij/download.html). The intraepidermal nerve fiber (IENF) density was expressed as the number of fibers/mm of epidermal length. In the distal leg, normative values from our laboratory (mean ± SD, 5th percentile) of IENF were 11.16 ± 3.70, 5.88 fibers/mm for subjects aged < 60 years and 7.64 ± 3.08, 2.50 fibers/mm for subjects aged ≥ 60 years.[15] Age- and gender-matched controls were retrieved from our previously described database.[9]

References

1. Cornblath DR, Asbury AK, Albers JW, et al. Research criteria for diagnosis of chronic inflammatory demyelinating polyneuropathy (CIDP). Neurology 1991;41:617-618.

2. Asbury AK, Cornblath DR. Assessment of current diagnostic criteria for Guillain-Barre syndrome. Ann Neurol 1990;27(Supp):S21-S24.

3. Slee M, Selvan A, Donaghy M. Multifocal motor neuropathy: The diagnostic spectrum and response to treatment. Neurology 2007;69:1680-1687.

4. Berg-Vos RM, Franssen H, Wokke JH, Van Es HW, van den Berg LH. Multifocal motor neuropathy: diagnostic criteria that predict the response to immunoglobulin treatment. Ann Neurol 2000;48:919-926.

5. Leger JM, Chassande B, Musset L, Meininger V, Bouche P, Baumann N. Intravenous immunoglobulin therapy in multifocal motor neuropathy: a double-blind, placebo-controlled study. Brain 2001;124:145-153.

6. Olney RK, Lewis RA, Putnam TD, Campellone JV, Jr. Consensus criteria for the diagnosis of multifocal motor neuropathy. Muscle Nerve 2003;27:117-121.

7. Rajkumar SV, Dispenzieri A, Kyle RA. Monoclonal gammopathy of undetermined significance, Waldenstrom macroglobulinemia, AL amyloidosis, and related plasma cell disorders: diagnosis and treatment. Mayo Clin Proc 2006;81:693-703.

8. Lin YH, Hsieh SC, Chao CC, Chang YC, Hsieh ST. Influence of aging on thermal and vibratory thresholds of quantitative sensory testing. J Peripher Nerv Syst 2005;10:269-281.

9. Pan CL, Tseng TJ, Lin YH, Chiang MC, Lin WM, Hsieh ST. Cutaneous innervation in Guillain-Barre syndrome: pathology and clinical correlations. Brain 2003;126:386-397.

10. Liu YT, Lee YC, Yang CC, Chen ML, Lin KP. Transthyretin Ala97Ser in Chinese-Taiwanese patients with familial amyloid polyneuropathy: genetic studies and phenotype expression. J Neurol Sci 2008;267:91-99.

11. Larkin MA, Blackshields G, Brown NP, et al. Clustal W and Clustal X version 2.0. Bioinformatics 2007;23:2947-2948.

12. Waterhouse AM, Procter JB, Martin DMA, Clamp M, Barton GJ. Jalview version 2--a multiple sequence alignment editor and analysis workbench. Bioinformatics 2009;25:1189-1191.

13. Hornberg A, Eneqvist T, Olofsson A, Lundgren E, Sauer-Eriksson AE. A comparative analysis of 23 structures of the amyloidogenic protein transthyretin. J Mol Biol 2000;302:649-669.

14. Hsieh YL, Chiang H, Tseng TJ, Hsieh ST. Enhancement of cutaneous nerve regeneration by 4-methylcatechol in resiniferatoxin-induced neuropathy. J Neuropathol Exp Neurol 2008;67:93-104.

15. Tseng MT, Hsieh SC, Shun CT, et al. Skin denervation and cutaneous vasculitis in systemic lupus erythematosus. Brain 2006;129:977-985.

Supplementary Results

Supplementary Figure 1 Deposition of transthyretin in amyloid on nerve biopsies.

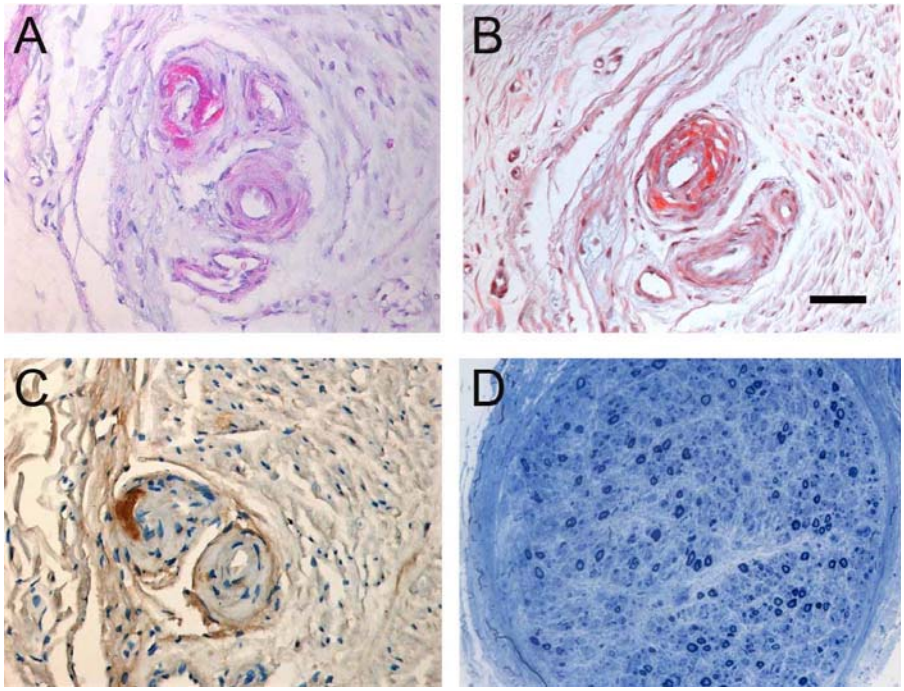

Sural nerve biopsies were stained with hematoxylin-eosin (A) and Congo red (B). Sections were further immunostained with anti-transthyretin antiserum (TTR, dark brown) and then counterstained with hematoxylin (blue) (C). Semi-thin sections were stained with toluidine blue (D).

(A) The amyloid appeared as eosinophilic aggregates near a blood vessel.

(B) On Congo red staining, the amyloid exhibited as red deposits around the vascular walls.

(C) The amyloid in the vascular wall contained TTR(+) aggregates.

(D) The nerve biopsy showed a pattern of axonal degeneration.

Bar, 40 μm for A~C, 62 μm for D.

Supplementary Figure 2. Skin denervation in amyloid neuropathy with mutated transthyretin (Ala97Ser)

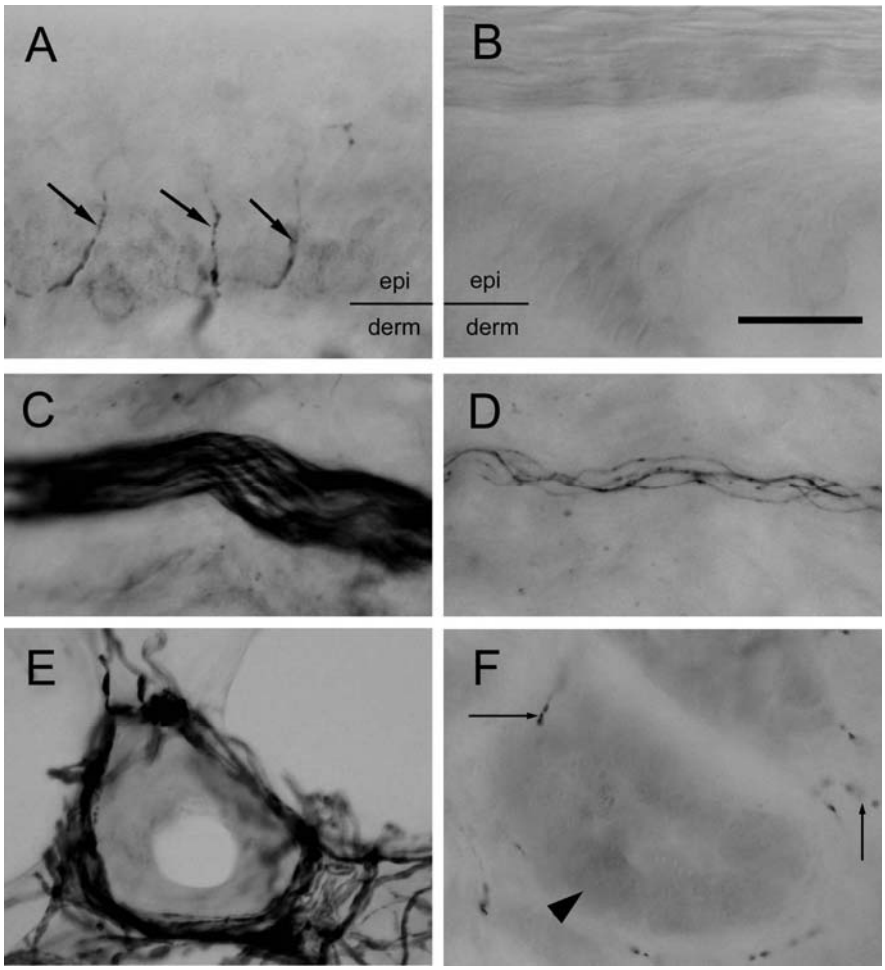

Skin sections were immunostained with anti-protein gene product (PGP) 9.5 in the controls (A, C, E) and Ala97Ser (B, D, F) for nerve fibers in the epidermis (epi) and dermis (derm).

(A) In the epidermis of the control skin, PGP 9.5 (+) intraepidermal nerve fibers (arrows) with a varicose appearance.

(B) Intraepidermal nerve fibers were depleted in an Ala97Ser patient.

(C) In the dermis of the control skin, nerve fibers in a nerve bundle appeared as dense immunoreactive lines.

(D) In an Als97Ser patient, dermal nerve fibers were markedly reduced in number and only some individual dermal nerve fibers appeared as fragmented lines.

(E) In the control skin, nerve fibers surrounded secretory coils of sweat glands.

(F) Innervation of sweat glands in Ala97Ser was almost completely absent and only some immunoreactive dots (arrows) in the surrounding of sweat coils (arrowhead) could be seen, which represented degenerated nerve fibers.

Bar, 30 μm

Supplementary Table 2. Nerve conduction studies and quantitative sensory testing

Patient no.	Amplitude		Threshold			SSR at sole	RRIV	
	Peroneal CMAP (mV)	Sural SAP (μV)	Warm (°C)	Cold (°C)	Vibratory (μm)		At rest (%)	Deep Breathing (%)
1	0.84	0	48	22	30.4	Abs	2.96	5.97
2	1.34	4.12	47.5	24.7	10.8	N	7.87 (N)	9.75 (N)
3	0	0	50	0	130.0	Abs	3.26	5.28
4	0	0	50	19.5	89.5	Abs	3.53	5.04
5	2.51 (N)	5.55 (N)	-	-	-	Abs	Arrhy	Arrhy
6	0.41	0	-	-	-	Abs	1.26	1.79
7	1.02	2.73	50	27 (N)	10.0	N	3.48	5.51
8	0	0	50	0	130.0	Abs	1.27	2.11
9	0.96	2.83	41.9 (N)	29.7 (N)	70.0	Abs	9.22 (N)	11 (N)
10	0	0	-	-	-	Abs	Arrhy	Arrhy
11	0.80	0	50	0	130.0	Abs	2.27	3.05
12	1.35	0	50	0	24.0	Abs	3.02	3.55
13	0	0	47	0	27.5	Abs	4.34	6.8
14	0.15	0	46.1	28 (N)	130.0	N	1.45	2.41
15	0.48	3.01	49	21.4	21.0	Abs	3.02	3.89
16	0	0	50	0	130.0	Abs	2.19	3.75
17	1.20	0	47.5	24.1	130.0	Abs	2.13	3.56
18	0.73	2.64	50	0	130	N	3.24	4.97
19	0.27	2.95	50	0	130	Abs	Arrhy	Arrhy
Summary	94.7%	94.7%	93.8%	81.2%	100%	78.9%	87.5%	87.5%

CMAP, compound muscle action potential; SAP, sensory action potential; Warm, warm threshold of the toe; Cold, cold threshold of the toe; Vibratory, vibratory threshold at the lateral malleolus; SSR: sympathetic skin response; RRIV: R-R interval variability; -, not done; N, within normal limits; Abs, absent response; Arrhy, Arrhythmia; Summary, abnormal rate for the laboratory examinations